

Future-Proofing Energy Infrastructure: Power Grid Risk Assessment



Muneer Qudaisat, Dela Houssou, William Gallus, and Alice Alipour

Contents

1	Introduction	1125
2	Climatic Parameters	1128
3	Maximum Wind Speeds and Electric Power Network Reliability	1130
4	Results and Conclusions	1133
	References	1134

1 Introduction

Uninterrupted power supply through robust power generation, transmission, and distribution in electric power networks (EPNs) is crucial to keep society functioning today. However, local power grids are prone to whims of weather events with undeniable impacts, such as hurricanes, strong winds, tornados, wildfires, floods, blizzards, or extreme cold. The profound impact of strong winds on power grids often leads to widespread disruptions in the electricity supply caused by breaking power lines, toppling utility poles, and damage to transmission towers [1, 2]; these threats, coupled with flying debris, pose a significant threat to the structural integrity of the grid. Extreme high or low temperatures are usually associated with higher electricity demand that can potentially overload the grid, leading to equipment failures and blackouts. For colder climates, extreme winter weather events such as ice storms and heavy wet snowfall can build up on power lines, weighing them down

M. Qudaisat · D. Houssou · W. Gallus · A. Alipour (✉)
Iowa State University, Ames, IA, USA
e-mail: muneerq@iastate.edu; alipour@iastate.edu

and potentially causing them to snap. Heavy rainfall accompanying hurricanes and organized thunderstorm systems, including derechos, can lead to riverine flood events or more local flash flooding, impacting substations and underground grids and weakening the foundation of poles and towers.

As climate change accelerates, its impact exacerbates the challenges faced by power grids in the burden of extreme weather events. Rising global temperatures may contribute to the intensification of hurricanes, increased frequency, and changes in the timing and location of wildfires and tornadoes. Additionally, shifting climate patterns may impact severe weather phenomena such as destructive winds brought by derechos. The warming climate also contributes to the instability of polar vortexes, escalating the likelihood of extreme cold spells. These climate-related shifts can change the frequency and severity of weather events, underscore the urgency of power grid infrastructure adaptation to the evolving challenges posed by a changing climate, and integrate more reliable power resources in the long run through effective climate change adaptation actions [3]. In the United States, 96% of power outages in 2020 were caused by severe weather events [4]. The increased intensity and frequency of natural hazards subsequently increased the consequences of such events on electric power networks. The adverse economic, social, and environmental impacts of power supply disruptions are significant. Preparing for the effects of these weather-related events is paramount to ensuring the resilience of power grids. Pre-emptive measures, such as reinforcing power lines and implementing smart grid technologies, can be strategically employed based on the insights provided by risk assessment. Moreover, the energy sector is essential to climate change vulnerability and adaptation analyses. It is responsible for almost two-thirds of greenhouse gas emissions and most power supply disruptions, causing adverse economic, social, and environmental impacts. Figure 1 shows weather events and their associated impacts on energy infrastructures [5].

Worldwide, the burden of global climate change and increasingly frequent associated events have started to affect various infrastructures, as highlighted by the UK Institution of Civil Engineers [6]. Much of climate change vulnerability, risk, and adaptation efforts are devoted to better understanding and quantifying global climate change impacts on the regional level, given the possibility of increasing the intensity and frequency of extreme environmental events, including intense wind events [7]. The investigation of the reliability of power networks is already challenging due to the numerous involved variables and their inherited uncertainties [8]; the estimation of climate change projections adds to the complexity of the process, especially the regional variability of climate, climate change, and infrastructure properties. Climate scientists use historical data and complex models to estimate and predict future environmental conditions. This process is usually region-dependent, as generalizing or adapting climate change adaptation strategies of other locations might not be feasible or possible due to the different and complex nature of climate change impacts and the critical infrastructure performance in each region [9], such as The North American Regional Climate Change Assessment Program (NARCCAP) [10]. High-resolution regional climate change projections

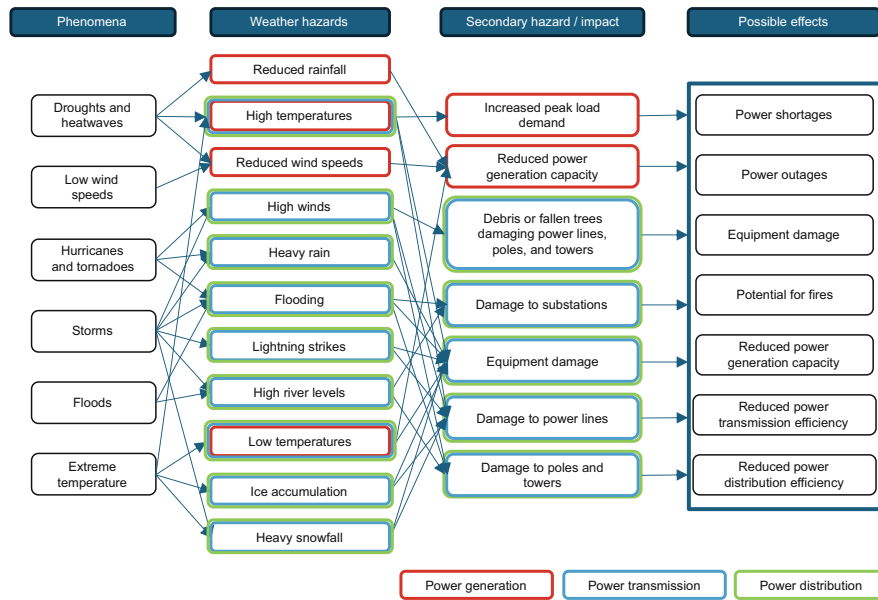


Fig. 1 Weather hazards and possible associated impacts on energy infrastructures

for the northeast USA developed using IPCC SRES emission scenarios by Hayhoe et al. [11], and for the Midwest area by Wuebbles et al. [12]. Additionally, regional projections have been developed in the UK (UK Climate Projection 2009 (UKCP09)) and KNMI climate change scenarios for the Netherlands 2006 following the fourth International Panel on Climate Change (IPCC) [13].

Numerous researchers have studied the future temperature, precipitation, and wind speed trends. Mideksa and Kallbekken investigated thermal power plants' supply sensitivity to temperature changes due to the large geographical variability [14]. Bloomfield et al. investigated the effects of the shifting climate on renewable energy resources and the supply-demand balance in future power systems [15]. Dobson et al. [16] addressed the power system blackouts and outages driven by extreme weather events and their future projections. The increasing ambient temperature associated with climate change and global warming compromises the efficiency and maximum capacity lifetime of power transformers and power lines, as they are vulnerable to high ambient air temperatures [17]. Global warming and, subsequently, ocean warming impact the complex process of wind formation, leading to changes in wind patterns and currents that can promote distribution network failure by rupturing the poles and wire lines, damaging pole-mounted equipment, or causing cascading outages [18]. Increasing participation intensity, storm surge events, and rising sea levels at some locations jeopardize the power transmission and distribution lines and substations to risk flooding [19–21].

2 Climatic Parameters

Based on the region, climate change can increase the imposed hazard on power distribution networks through increasing extreme wind speeds each year, hence making the grid assets more prone to failure, increasing temperature that expedites the decay rate of wooden poles and increases their vulnerability with time. However, annual rainfall reduction can slow the decay rate of wooden poles [22]. Therefore, assessing the impact of climate change on power distribution networks requires detailed modeling to capture the contrasting region-dependent effects of climatic changes and their differing extents. To visibly measure the effect of projected regional climate change on EPNs' performance, the baseline vulnerability status of a network needs to be established first. Hence, a case study of four cities in Iowa in the USA, namely, Muscatine, Algona, Pella, and Cedar Falls, is presented.

The WRF 3.4.1 model is a numerical weather prediction system designed to serve atmospheric research and operational forecasting needs, therefore assessing the infrastructure resilience from multiple aspects [23]. This study uses a higher resolution 4 km cell grid than is typically used operationally to give a more accurate projection for frequency and intensity of wind speed, precipitation (flooding), and freezing rain over the 13-year simulation period considering climate change. The resolution used herein is much finer compared to the 18 km resolution used in earlier models, including the UK flooding model (UKCP 18), global reanalysis (ERA5), Global-to-Regional Integrated Forecast System (GRIST), China Merged Precipitation Analysis (CMPA), and Integrated Multi-Satellite Retrievals for the Global Precipitation Measurement (IMERG) [24, 25]. The simulation period is based on a reference control period spanning from October 1, 2000, to September 30, 2013, with 6 hours and 0.7 °C and a sensitivity model considering the effects of climate change using the PWG approach (“Physics-WGNE” (Working Group on Numerical Experimentation)), with ten perturbed physical fields to account for uncertainties climate system mechanism. The future climate simulation extends from October 1, 2086, to September 30, 2099.

2.1 Maximum Wind Speed

The behavior of the wind speed shows oscillation around a mean value. Still, given the turbulent characteristic of wind, the maximum wind speed can peak away from the mean value [26]. The wind speed dataset contains maximum wind speeds 10 meters above ground level. Structural analysis showed that poles start to fail near the 15 m/s wind speed threshold, considering that the model values are averaged over the 4×4 km box and peak winds usually are very localized. In addition, models typically are deficient in bringing momentum to the ground. Accordingly, the projections of wind speed over 20 m/s were calculated along with their frequencies in the control and future models.

2.2 Wind Speed Simulation Results

The following Fig. 2 shows the high winds of the four study areas during the reference and projected years. There is a noticeable variety in high wind speeds across the four regions. At the same time, some areas experience higher wind speeds, indicating natural weather pattern fluctuation that can be attributed to terrains and other landscape features. For example, Muscatine generally has higher wind speeds over the years, and occasional years, such as 2090 and 2091, show significant increases in peak wind speeds. Compared to earlier years, Algona shows increased peak wind speeds in certain future years, such as 2087 and 2092, and Pella shows increased peak wind speeds in certain years, such as 2090 and 2093. Cedar Falls has less wind speed fluctuation across the study years. Hence, specific years exhibit extremely high wind speeds compared to the average, indicating the possibility of intermittent extreme weather events, and there seems to be a trend of stronger winds toward the later years of the dataset.

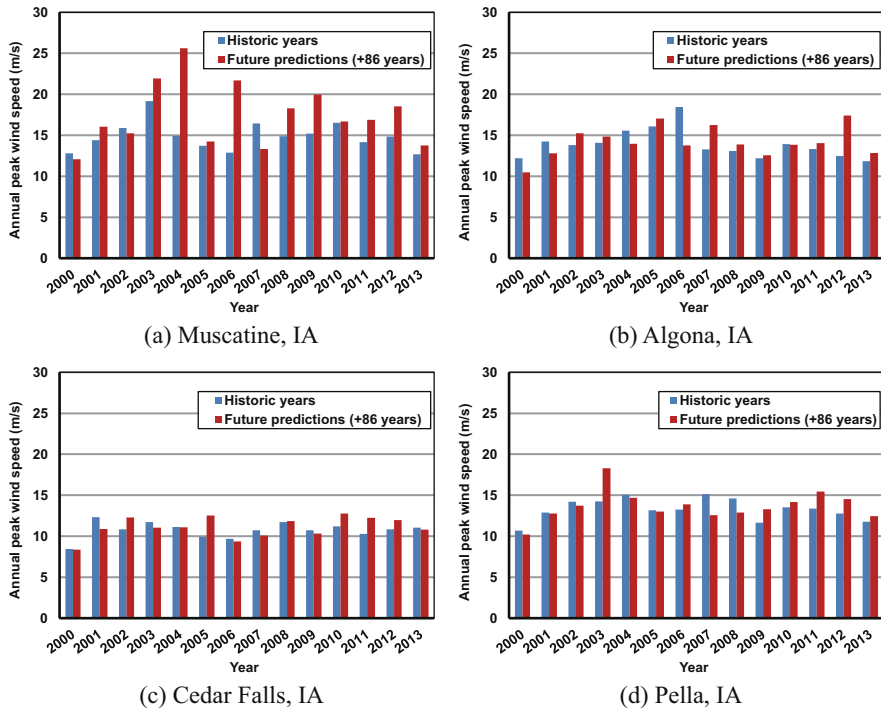


Fig. 2 Maximum wind speed in the case study areas. (a) Muscatine, IA. (b) Algona, IA. (c) Cedar Falls, IA. (d) Pella, IA

3 Maximum Wind Speeds and Electric Power Network Reliability

3.1 System Fragility Curve Development

The radial configuration of local power distribution networks leads to service outage downstream from any interruption point, i.e., network component failure. Hence, it is crucial to investigate the reliability of the network components in correspondence to various environmental event intensities. In this study, which focuses on the wooden power distribution poles, the capacity of those poles is influenced by their class, geometry, age, and the environmental conditions that expedite their deterioration. After analyzing the wind demand on the poles in the network and their capacity, it is essential to use a limit state function to describe the system's vulnerability by establishing the pole's conditional failure probability in response to increasing wind speed.

3.2 Wind Demand on EPN Components

The poles and wires of EPNs are directly exposed to wind and flying debris. Hence, they are considered highly vulnerable. To evaluate the exerted wind loads, the following relationships provided by ASCE/SEI 7-22 can be used [27]:

$$F = 0.613 K_z K_{zt} K_d K_e G C_f A_f V^2 \text{ (N)} \quad (1)$$

G is the gust-effect factor, C_f is the force coefficient, A_f is the pole or wire area projected normal to the wind direction. K_z is the velocity pressure exposure coefficient, K_{zt} is a topographic factor, and K_d is the wind directionality. K_e is the ground elevation factor. V is the basic 3-sec gust wind speed. The distributions and coefficient of variations (CoV) of the mentioned random variables related to poles and wires are summarized by Ellingwood and Tekie [28].

3.3 EPN Components Capacity and Case Study

The vast majority of US power distribution poles are wooden due to the availability, serviceability, and lower wood cost than other pole materials [29]. The American National Standards Institute published in (ANSI-O5.1) classified wooden poles into 15 classes designed to have approximately the same load-carrying capacity regardless of their species [30]. In the four locations where the wind speed projections were analyzed, the main wood pole is the Class 3 Southern pine pole. Hence, a fragility function for a 40-year-old Class 3 pole with an average height of 13 meters and an average wire span of 100 meters is chosen as an example.

3.4 Limit State Function

The wind loads acting on the poles and wires of EPNs translate into bending moment in the pole and tensile stress in the wires; hence, the structural demand is directly proportional to wind speed and duration. On the other hand, the EPNs can be structurally analyzed to determine the structural capacity of their components in response to various weather events and external stresses. The following relationship can generally describe the limit state function, $G(x)$:

$$G(x) = C(x_c, d_c) - D(x_d, d_d) \quad (2)$$

Where C is the structural capacity as a function of random and deterministic variables x_c and d_c , respectively. D is the structural demand on the system as a function of random and deterministic variables x_d and d_d , respectively. The system fails whenever the demand exceeds the system capacity and results in the limit state function being negative. The Latin hypercube sampling method (LHS) is used to generate ten thousand random samples for wind speeds, which are used in accordance with the provisions of ASCE/SEI 7-22 to calculate wind load on the poles and connected wires. Subsequently, the failure probability at each wind speed.

3.5 Fragility Function Development

After structurally analyzing the ten thousand realizations and determining their failure or survival based on the limit state function for three modes of failure, i.e., pole rupture, foundation failure, and wires breakage, The pole rupture turned out to be the predominant mode of failure within the range of wind speeds in this study. Afterward, the log-normal distribution was chosen to describe the relationship between wind speed and the fragility of the poles. The distribution parameters can be obtained using the maximum likelihood estimation (MLE) method [31, 32]. The following fragility function shows an increasing failure probability of the pole with increasing wind speeds. Considering the generally projected increase in wind speed in some regions in the coming years, accompanied by the degradation of wooden poles and strength decay, accounting for climate change impacts becomes necessary (Fig. 3).

3.6 The Annual Probability of Failure

The annual probability of failure is obtained by performing a mathematical convolution of the fragility and hazard curve; the last describes the instantaneous probability of failure at a given wind speed. The wind speed occurrence frequency is

Fig. 3 Fragility function of a 13 m high Class 3 wooden pole

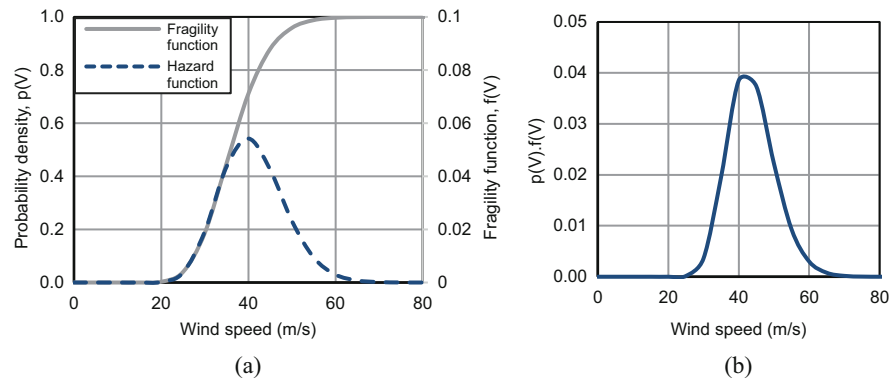
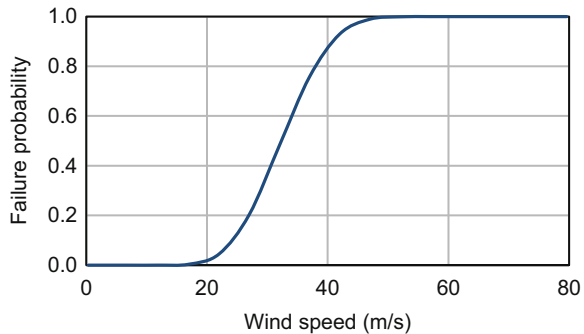


Fig. 4 (a) Fragility and hazard curves, (b) fragility and hazard functions convolution curve

presented through a probability density function (PDF) that models the available location-related wind data based on the data provided by Vickery et al. [33] in Fig. 4a. Convolution principally combines the fragility and hazard functions to show the overall likelihood of failure at different wind speeds throughout the year. The annual probability of failure, P_f , at maximum wind speed, V_{\max} , can be expressed as:

$$P_f = \int_0^{V_{\max}} p(V).f(V).dV \quad (3)$$

where $p(V)$ is the fragility curve, representing the probability of failure at wind speed V , and $f(V)$ represents the PDF of wind speed V , obtained from the hazard curve. Hence, the annual probability of failure, P_f , is the area under the curve in Fig. 4b up to the maximum wind speed, V_{\max} .

Considering the prevailing wind conditions, the change in the annual probability of failure of the pole between the reference year and the projected year offers further insight into the changing risk of failure associated with climate change, as depicted in Fig. 5. Despite the shown fluctuations and lack of a clear linear trend between the

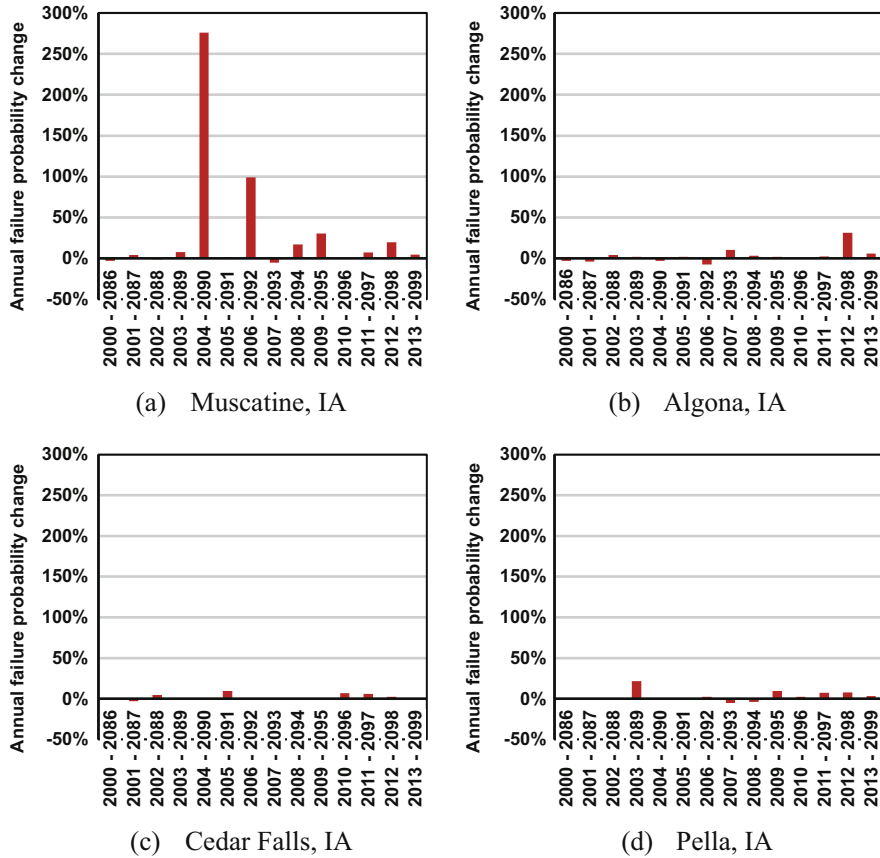


Fig. 5 Percent change of the annual failure probability in the case study areas. **(a)** Muscatine, IA. **(b)** Algona, IA. **(c)** Cedar Falls, IA. **(d)** Pella, IA

change in annual failure probability over the years, there were substantial increases, such as 275% in 2090 for Muscatine, and other decreases, such as -8% in 2092 for Algona. It can be noticed that those percentages correspond to the projected change in maximum wind speed displayed in Fig. 2 as increasing wind speed increases the wind load demand and, subsequently, the component failure probability.

4 Results and Conclusions

As the intensity and frequency of some weather events increase, it further stresses the power supply chain integrity. Distribution networks are the most vulnerable to extreme weather events as they can cause widespread power outages, overload the grid, and potentially lead to equipment failure. Fragility models are essential to

estimate the likelihood of component failure and risk assessment, enabling informed decision-making for predictive maintenance and risk mitigation procedures. This research reviewed the impacts of the ongoing climate change on power distribution networks by estimating the projected maximum wind speeds, evaluating their effect on the components of the power distribution network, and establishing the vulnerability of the EPN as a function of wind speed through statistical analysis. The presented research discusses weather phenomena, their association with climate change, and their projected impacts. The numerical weather prediction model WRF 3.4.1 with a 4 km resolution cell grid gives a more accurate projection of the frequency and intensity of high winds. The percent change in the predicted annual probability of failure is associated with the percent increase or decrease of the high wind speed, therefore calling for adaptive and continuous risk assessment of the network to ensure its reliability.

References

1. Dikshit, S., Dobson, I., Alipour, A.: Cascading structural failures of towers in an electric power transmission line due to straight line winds. *Reliab. Eng. Syst. Saf.* **250**, 110304 (2024) <https://doi.org/10.1016/j.ress.2024.110304>
2. Alipour, A., Sarkar, P., Dikshit, S., Razavi, A., Jafari, M.: Analytical approach to characterize tornado-induced loads on lattice structures. *J. Struct. Eng.* **146**(6), (2020) [https://doi.org/10.1061/\(ASCE\)ST.1943-541X.0002660](https://doi.org/10.1061/(ASCE)ST.1943-541X.0002660)
3. Dumas, M., Kc, B., Cunliff, C.I.: Extreme weather and climate vulnerabilities of the electric grid: a summary of environmental sensitivity quantification methods. 2019 Aug 1 [cited 2024 Mar 12]; Available from: <http://www.osti.gov/servlets/purl/1558514/>
4. Stone, B., Mallen, E., Rajput, M., Gronlund, C.J., Broadbent, A.M., Krayenhoff, E.S., et al.: Compound climate and infrastructure events: how electrical grid failure alters heat wave risk. *Environ. Sci. Technol. [Internet]*. **55**(10), 6957–6964 (2021) [cited 2024 Mar 13]) Available from: <https://www.apmresearchlab.org/10x-power-climate>
5. Gonçalves, A.C.R., Costoya, X., Nieto, R., Liberato, M.L.R.: Extreme weather events on energy systems: a comprehensive review on impacts, mitigation, and adaptation measures. *Sustain. Energy Res. [Internet]*. **11**(1), 4 (2024) Available from: <https://jrenewables.springeropen.com/articles/10.1186/s40807-023-00097-6>
6. Knutti, R.: Should we believe model predictions of future climate change? *Philos. Trans. R. Soc. A Math. Phys. Eng. Sci.* **366**(1885), 4647–4664 (2008) Available from: <https://royalsocietypublishing.org/doi/10.1098/rsta.2008.0169>
7. Della-Marta, P.M., Mathis, H., Frei, C., Liniger, M.A., Kleinn, J., Appenzeller, C.: The return period of wind storms over Europe. *Int. J. Climatol.* **29**(3), 437–459 (2009)
8. Micheli, L., Alipour, A., Laflamme, S.: Multiple-surrogate models for probabilistic performance assessment of wind-excited tall buildings under uncertainties. *ASCE-ASME Journal of Risk and Uncertainty in Engineering Systems Part A: Civil Engineering* **6**(4), (2020) <https://doi.org/10.1061/AJRUA6.0001091>
9. Ryan, P.C., Stewart, M.G.: Regional variability of climate change adaptation feasibility for timber power poles. *Struct. Infrast. Eng. [Internet]*. **17**(4), 579–589 (2021) Available from: <https://www.tandfonline.com/doi/full/10.1080/15732479.2020.1843505>
10. Mearns, L.O., Gutowski, W., Jones, R., Leung, R., McGinnis, S., Nunes, A., et al.: A regional climate change assessment program for North America. *Eos (Washington DC)*. **90**(36), 311 (2009)

11. Hayhoe, K., Wake, C., Anderson, B., Liang, X.Z., Maurer, E., Zhu, J., et al.: Regional climate change projections for the Northeast USA. *Mitig. Adapt. Strateg. Glob. Chang.* [Internet]. **13**(5–6), 425–36 (2008 [cited 2024 Mar 10]) Available from: <https://link.springer.com/article/10.1007/s11027-007-9133-2>
12. Wuebbles, D.J., Hayhoe, K.: Climate change projections for the United States Midwest. *Mitig. Adapt. Strateg. Glob. Chang.* [Internet]. **9**(4), 335–63 (2004 Oct [cited 2024 Mar 10]) Available from: <https://link.springer.com/article/10.1023/B:MITI.0000038843.73424.de>
13. Van Den Hurk, B., Klein Tank, A., Lenderink, G., Van Ulden, A., Van Oldenborgh, J., Katsman, C., et al.: KNMI Climate Change Scenarios 2006 for the Netherlands [Internet]. 2006. Available from: www.knmi.nl
14. Mideksa, T.K., Kallbekken, S.: The impact of climate change on the electricity market: a review. *Energy Policy*. **38**(7), 3579–3585 (2010)
15. Bloomfield, H.C., Brayshaw, D.J., Troccoli, A., Goodess, C.M., De Felice, M., Dubus, L., et al.: Quantifying the sensitivity of european power systems to energy scenarios and climate change projections. 2020 [cited 2024 Mar 10]; Available from: <http://creativecommons.org/licenses/by/4.0/>
16. Dobson, I., Dong, Y., Kezunovic, M.: Impact of extreme weather on power system blackouts and forced outages: new challenges. [cited 2024 Mar 11]; Available from: <https://www.researchgate.net/publication/228379681>
17. Wilbanks, T.J., Fernandez, S.J.: Climate Change and infrastruCture, urban systems, and Vulnerabilities Technical Report for the US Department of Energy in Support of the National Climate Assessment national Climate assessment regional technical input report series
18. Fern, S.J., et al.: Application of hybrid geo-spatially granular fragility curves to improve power outage predictions. *J. Geograph. Nat. Disast.* [Internet]. **4**(2), 1–6 (2014 [cited 2024 Mar 12]) Available from: <https://www.longdom.org/open-access/application-of-hybrid-geospatially-granular-fragility-curves-to-improve-power-outage-predictions-33876.html>
19. Zamuda, C., Mignone, B., Bilello, D., Hallett, K.C., Lee, C., Macknick, et al.: US Department of Energy. US Energy Sector Vulnerabilities to Climate Change and Extreme Weather (2013 [cited 2024 Mar 11]) Available from: <https://apps.dtic.mil/sti/citations/ADA583709>
20. Zhang, N., Alipour, A.: Flood risk assessment and application of risk curves for design of mitigation strategies. *Int. J. Crit. Infrastructure Prot.* **36**, 100490 (2022) <https://doi.org/10.1016/j.ijcip.2021.100490>
21. Zhang, N., Alipour, A.: A two-level mixed-integer programming model for bridge replacement prioritization. *Abstract. Comput.-Aided Civ. Infrastruct. Eng.* **35**(2), 116–133 (2020) <https://doi.org/10.1111/mice.v35.2>; <https://doi.org/10.1111/mice.12482>
22. Hsiang, W.C., Wang, X.: Vulnerability of timber in ground contact to fungal decay under climate change. *Clim. Change* [Internet]. **115**(3–4), 777–794 (2012) Available from: <http://link.springer.com/10.1007/s10584-012-0454-0>
23. Zhang, G., Zhang, F., Wang, X., Zhang, X.: Fast resilience assessment of distribution systems with a non-simulation-based method. *IEEE Trans. Power Deliv.* [Internet]. **37**(2) (2022) Available from: <https://doi.org/10.1109/TPWRD>
24. Chen, T., Li, J., Zhang, Y., Chen, H., Li, P., Che, H.: Evaluation of hourly precipitation characteristics from a global reanalysis and variable-resolution global model over the Tibetan Plateau by using a satellite-gauge merged rainfall product. *Remote Sens.* **15**(4), 1013 (2023)
25. Liu, H., Liu, X., Liu, C., Yun, Y.: High-resolution regional climate modeling of warm-season precipitation over the Tibetan Plateau: impact of grid spacing and convective parameterization. *Atmos. Res.* **281**, 106498 (2023)
26. Teoh, Y.E., Alipour, A., Cancelli, A.: Probabilistic performance assessment of power distribution infrastructure under wind events. *Eng. Struct.* **15**, 197 (2019)
27. Structural Engineering Institute: Minimum Design Loads and Associated Criteria for Buildings and Other Structures [Internet], p. 593. American Society of Civil Engineers, Reston (2021) Available from: <https://ascelibrary.org/doi/book/10.1061/9780784415788>

28. Ellingwood, B.R., Tekie, P.B.: Wind load statistics for probability-based structural design. *J. Struct. Eng.* [Internet]. **125**(4), 453–463 (1999) Available from: <https://ascelibrary.org/doi/10.1061/%28ASCE%290733-9445%281999%29125%3A4%28453%29>
29. Mohammadi Darestani, Y., Shafeezaeh, A.: Multi-dimensional wind fragility functions for wood utility poles. *Eng. Struct.* **183**, 937–948 (2019)
30. American National Standard for Telecommunications Wood Poles-Specifications & Dimensions [Internet]. 2009 [cited 2023 Jun 7]. Available from: <https://webstore.ansi.org/standards/ansi/ansi052022>
31. Shinozuka, M., Feng, M.Q., Lee, J., Naganuma, T.: Statistical analysis of fragility curves. *J. Eng. Mech.* [Internet]. **126**(12), 1224–1231 (2000) Available from: <https://ascelibrary.org/doi/10.1061/%28ASCE%290733-9399%282000%29126%3A12%281224%29>
32. Dikshit, S., Alipour, A.: A moment-matching method for fragility analysis of transmission towers under straight line winds. *Reliab. Eng. Syst. Saf.* **236**, 109241 (2023) <https://doi.org/10.1016/j.ress.2023.109241>
33. Vickery, P.J., Wadhera, D., Galsworthy, J., Peterka, J.A., Irwin, P.A., Griffis, L.A.: Ultimate wind load design gust wind speeds in the United States for use in ASCE-7. *J. Struct. Eng.* [Internet]. **136**(5), 613–625 (2010) Available from: <https://ascelibrary.org/doi/10.1061/%28ASCE%29ST.1943-541X.0000145>

Open Access This chapter is licensed under the terms of the Creative Commons Attribution 4.0 International License (<http://creativecommons.org/licenses/by/4.0/>), which permits use, sharing, adaptation, distribution and reproduction in any medium or format, as long as you give appropriate credit to the original author(s) and the source, provide a link to the Creative Commons license and indicate if changes were made.

The images or other third party material in this chapter are included in the chapter's Creative Commons license, unless indicated otherwise in a credit line to the material. If material is not included in the chapter's Creative Commons license and your intended use is not permitted by statutory regulation or exceeds the permitted use, you will need to obtain permission directly from the copyright holder.

